Passive TCF Compensation in High Q Silicon Micromechanical Resonators

A.K. Samarao, G. Casinovi and F. Ayazi

IEEE International Conference on Micro Electro Mechanical Systems
pp. 116–119, January 2010

Abstract

This paper reports on passive temperature compensation techniques for high quality factor (Q) silicon microresonators based on engineering the geometry of the resonator and its material properties. A 105 MHz concave silicon bulk acoustic resonator (CBAR) fabricated on a boron-doped substrate with a resistivity of 10^{-3} Ω-cm manifests a linear temperature coefficient of frequency (TCF) of –6.3 ppm/˚C while exhibiting a Q of 101,550 ($fQ = 1.06\times10^{13}$). The TCF is further reduced by engineering the material property via a wafer-level aluminum thermomigration process to –3.6 ppm/˚C while maintaining an fQ of over 4×10^{12}. Such high fQ products with low TCF values are being reported for the first time in silicon and are critical for successful insertion of these devices into low-power low-phase noise frequency references and high performance resonant sensors.

Copyright Notice

PASSIVE TCF COMPENSATION IN HIGH Q SILICON MICROMECHANICAL RESONATORS

A.K. Samarao, G. Casinovi and F. Ayazi
Georgia Institute of Technology, Atlanta, Georgia, USA

ABSTRACT

This paper reports on passive temperature compensation techniques for high quality factor (Q) silicon microresonators based on engineering the geometry of the resonator and its material properties. A 105 MHz concave silicon bulk acoustic resonator (CBAR) fabricated on a boron-doped substrate with a resistivity of 10^{-3} Ω-cm manifests a linear temperature coefficient of frequency (TCF) of –6.3 ppm/°C while exhibiting a Q of 101,550 ($fQ = 1.06\times10^{13}$). The TCF is further reduced by engineering the material property via a wafer-level aluminum thermomigration process to –3.6 ppm/°C while maintaining an fQ of over 4×10^{12}. Such high fQ products with low TCF values are being reported for the first time in silicon and are critical for successful insertion of these devices into low-power low-phase noise frequency references and high performance resonant sensors.

INTRODUCTION

Silicon micromechanical resonators are being touted as an integrated alternative to the currently prevalent quartz resonators in timing and frequency control applications owing to their small form factor, ease of integration with CMOS circuitry and very high fQ product. Both capacitive [1] and piezoelectric [2] methods of transduction are being increasingly employed in silicon micromechanical resonators. However, the native TCF of approximately –30 ppm/°C in silicon is significantly larger in magnitude than that of the worst AT-cut quartz resonator [3]. Though active compensation techniques that electronically compensate the TCF have been demonstrated, passive techniques that do not consume additional power and chip area are of great interest. The most common passive temperature compensation technique in silicon micromechanical resonators is based on the use of composite structures consisting of materials whose stiffness changes in opposite ways with temperature. This approach dates back at least to the early 1980's [4], but is still the object of much active research. The main disadvantage of this approach is that the composite structure usually incorporates thin films of amorphous material on the silicon microresonator, and this has the effect of degrading the quality factor of the resonator [5].

In this work, capacitive silicon micromechanical resonators are used as a test vehicle to demonstrate a reduction in TCF of native silicon. Our group has been studying silicon bulk acoustic resonators (SiBARs) [1], which consist of a long rectangular bar resonating element placed between two electrodes, and supported symmetrically by two narrow support elements on the sides (Figure 1(a)). A DC polarization voltage (V_p) applied to the resonator generates an electrostatic field in the narrow capacitive gaps between the resonator and the electrodes. When an AC voltage is applied to the drive electrode, the resulting time-varying electrostatic force applied to the corresponding face of the resonator induces an acoustic wave that propagates through the bar, resulting in a width-extensional resonance mode (Figure 1(b)) whose frequency is primarily defined by width (W) of the SiBAR. Small changes in the air gap on the other side of the device induce a voltage on the sense electrode whose amplitude peaks at the mechanical resonance frequency.

Such an electrode and resonator design results in a uniform tensile force (F_Y along [110]) being applied along the entire length L of the resonator. The resulting width-extensional mode (WEM) is made up predominantly of longitudinal waves propagating along the width of the resonator. The Young's modulus (E) that determines the resonance frequency possesses a negative temperature coefficient, which causes the stiffness and thereby the frequency of the silicon resonators to decrease with increasing temperature. Although the linear thermal expansion coefficient (α) of silicon also contributes to the TCF, its contribution is negligible compared to the temperature coefficient of Young's modulus (TCE).

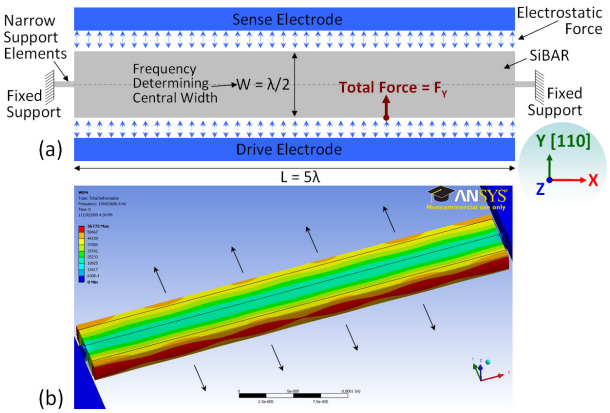

Figure 1: (a) Schematic and (b) simulated width-extensional mode of a conventional rectangular Silicon Bulk Acoustic Resonator (SiBAR).

Recently we reported on a temperature compensation technique for silicon resonators via degenerate doping wherein the effect of free charge carriers on the elastic constants of silicon were utilized to achieve a reduction in TCE [6]. In addition to such an engineering of the material properties of the resonator, this work demonstrates that modifying the geometry of the resonator and its actuation electrodes can effect an interaction between various types of acoustic waves that inherently minimizes the TCF of a silicon microresonator.

TCF REDUCTION BY ENGINEERING RESONATOR GEOMETRY

The momentary strain produced in the crystal lattice of the SiBAR by the propagation of longitudinal waves of the WEM distorts the equivalent energy levels of its electronic band structure [7]. As a consequence, the free charge carriers in silicon flow towards more energetically

favorable energy levels thereby shifting the Fermi level. The amount of free charge carrier flow and the resulting shift in Fermi level (and the total electronic energy) increases with temperature. The principle of conservation of energy requires that such temperature dependent change in the electronic energy of the system manifest itself as a corresponding temperature dependent change in the elastic energy of the system, which causes a negative TCE in silicon. However, by creating a relatively large strain in the resonating microstructure, the effect of strain from the WEM can be made minimal in comparison, thereby achieving temperature compensation. Such a large strain can be created by engineering the resonator geometry to excite additional longitudinal and shear acoustic waves in the resonator along with the longitudinal waves of the WEM.

Figure 2(a) introduces the Concave Silicon Bulk Acoustic Resonator (CBAR), which is realized by curving the long edges of the conventional rectangular SiBAR (Figure 1(a)) such that the central width remains λ/2 but the resonator has wider flanks on either side. The electrodes are designed with the same curvature as that of the CBAR. The normal electrostatic force applied to the curved CBAR surface by the electrodes can be resolved into its corresponding F_Y and F_X components as illustrated in Figure 2(a). The ensemble of the F_Y force components actuates the WEM of the CBAR along the Y (i.e., [110]) direction. The CBAR structure supports the WEM around the narrow central region as illustrated in Figure 2(b), at a resonance frequency determined by the central width λ/2. Hence the drive/sense electrodes are positioned around the actively transducing central region and not along the entire length of the CBAR. It was found that when the flank widths were made exactly equal to 3λ/4, almost all of the acoustic energy could be concentrated near the active central region with minimal acoustic energy at the flanks. Such resonator geometry minimizes the acoustic loss at the narrow support elements thereby enhancing the Q of the resonator.

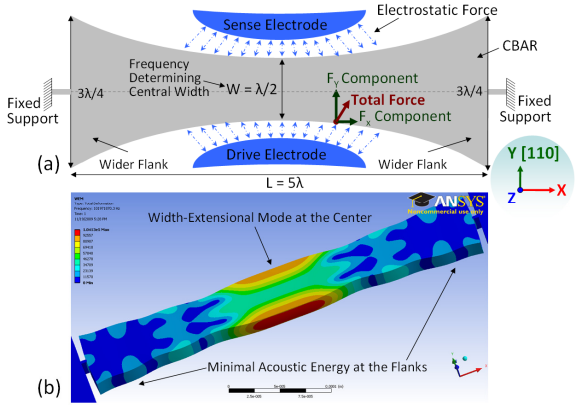

Figure 2: (a) Schematic and (b) simulated width-extensional mode of a Concave Silicon Bulk Acoustic Resonator (CBAR).

Figure 3 compares the longitudinal and shear strain in a SiBAR and CBAR. Figure 3(a) shows an increased longitudinal strain along *Y* direction in the WEM of the CBAR compared to that of the SiBAR. This is due to the concentration of acoustic energy near the center in a CBAR at a flank width of 3λ/4. Figures 3(b) and 3(c) confirm that the SiBAR structure has no additional strain components other than that produced by the WEM along the Y direction. In the case of a CBAR, the ensemble of F_X force components (Figure 2(a)) excites longitudinal waves (and thereby longitudinal strain) along the X direction (Figure 3(b)) and also contributes to shear waves (and thereby shear strain) along the XY plane (Figure 3(c)). All the strain components are excited by the same time-varying electrostatic forces from the drive electrode and therefore are in-phase. Hence, the additional strain components directly add on to the longitudinal strain produced by the WEM of the CBAR, rendering the effect of the latter on the electronic band structure minimal. As a result, this causes a reduction in TCF in the CBAR resonator geometry as compared to that of a SiBAR.

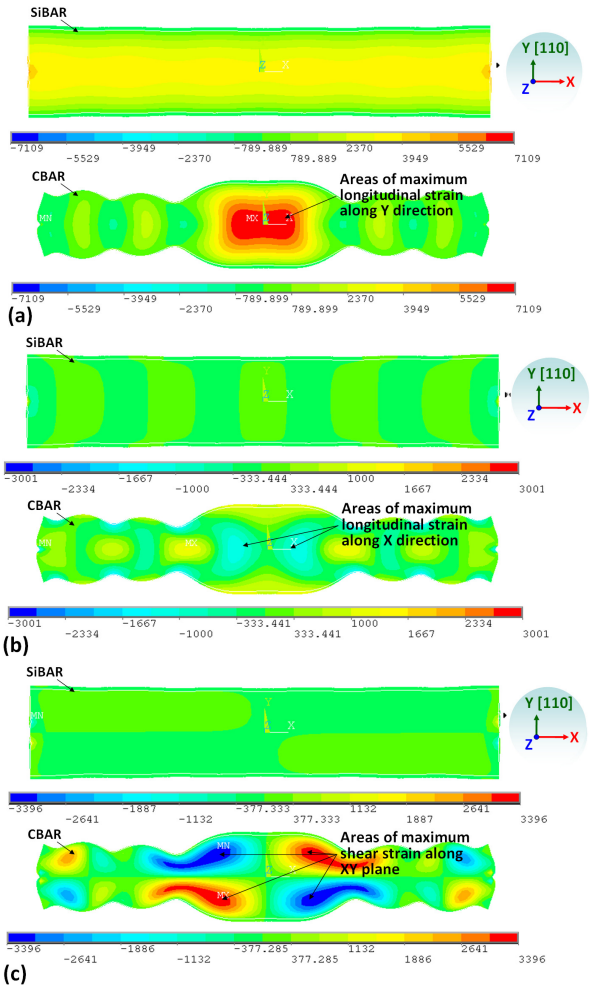

Figure 3: Simulated longitudinal strain along (a) Y and (b) X axes and shear strain along the (c) XY plane of SiBAR vs CBAR.

To demonstrate TCF reduction and Q enhancement, 100 MHz SiBAR and CBAR were fabricated on the same boron-doped silicon with a resistivity of ~10^{-3} Ω-cm using the HARPSS process [1] with a capacitive gap of 100 nm (Figure 4). The devices were measured in vacuum at a polarization voltage (V_P) of 10V and an input power level of -10 dBm. As shown in Figure 5, the TCF of the CBAR is measured to be −6.31 ppm/°C, which is 15 ppm/°C smaller than a SiBAR fabricated on the same wafer. The values of TCF were found to be consistent across several devices. Further, the measured response of the CBAR in vacuum (Figure 6) shows a Q of 101,550 at 104.92 MHz, which makes it the first silicon micromechanical resonator

reported with a TCF as low as −6.31 ppm/°C while maintaining an *fQ* product of over 1.06×10^{13}.

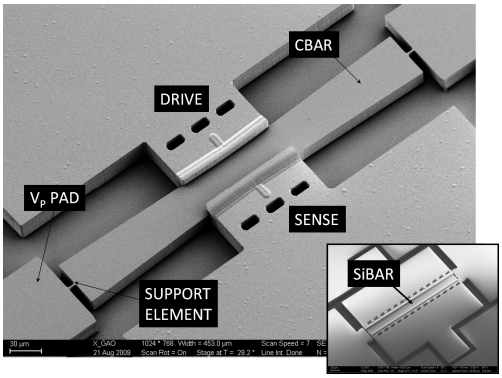

Fig 4: SEM image of) a Concave SiBAR (CBAR) with central width 40 µm (λ/2); flank width = 60 µm (3λ/4); thickness = 20 µm and length = 400 µm, fabricated on a ~10^{-3} Ω-cm silicon (Inset shows a conventional SiBAR).

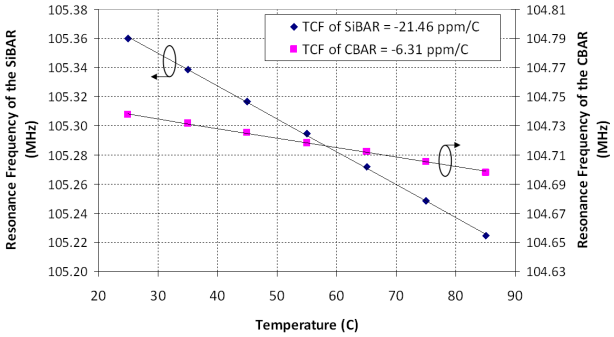

Fig 5: Measured TCF of SiBAR & CBAR fabricated on a ~10^{-3}Ω-cm wafer.

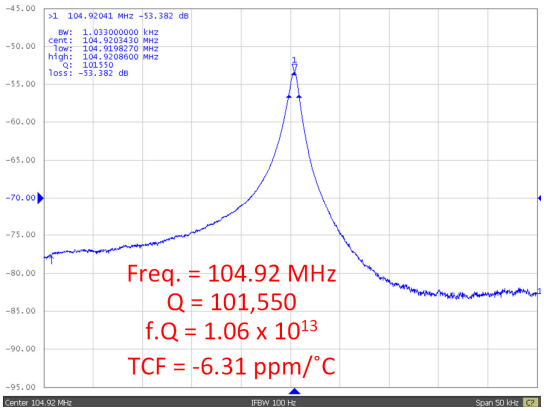

Fig 6: Measured frequency response in vacuum of a CBAR fabricated on a ~10^{-3}Ω-cm wafer.

To assess the influence of the ultra-low resistivity substrate on the achieved TCF values, the SiBAR and CBAR were also fabricated on a boron-doped wafer with very high resistivity of >1000 Ω-cm. Such a CBAR measured a TCF of −20.77 ppm/°C, which is still 12 ppm/°C smaller than the measured TCF of a SiBAR fabricated on the same wafer (Figure 7). This confirms that engineering of the resonator geometry is a viable passive technique for achieving TCF compensation in silicon micromechanical resonators with a possibility of simultaneous Q enhancement. A comparison of Figures 5 and 7 shows a larger percentage of TCF reduction from SiBAR to CBAR in very low-resistivity boron-doped silicon. Additional strain in the silicon lattice due to the very high concentration of boron atoms is suspected to add to the existing strain components in CBAR to effect a larger reduction in TCF.

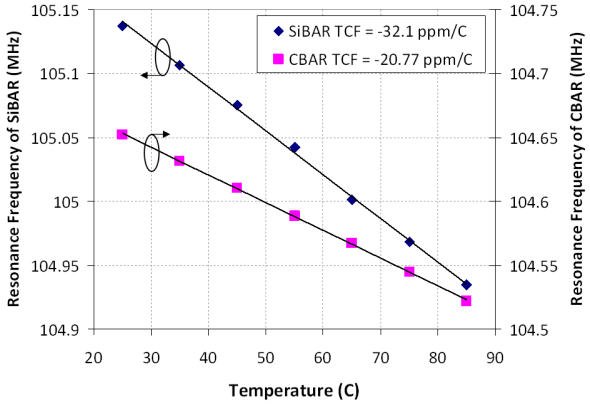

Fig 7: Measured TCF of SiBAR & CBAR fabricated on a >1000 Ω-cm wafer.

TCF REDUCTION BY ENGINEERING MATERIAL PROPERTY

By comparing the TCF of the SiBARs (or CBARs) from Figures 5 and 7, the reduction in TCF with the reduction in silicon resistivity via boron-doping is evident. The introduction of a dopant like boron that has an atomic radius smaller than silicon creates a large shearing strain in the silicon lattice. We reported in [6] that degenerate levels of doping with a boron concentration of ~ 2×10^{20} atoms/cm^3 (i.e., < 10^{-4} Ω-cm) generate sufficiently large shearing strain, compared to the longitudinal strain of the WEM, to reduce the TCF to −1.5 ppm/°C in SiBARs. Thus, the material property of a silicon resonator can be engineered via doping to achieve a reduction in TCF. However, the duration of boron doping to reduce the resistivity in silicon from the commercially available 10^{-2} Ω-cm to ultra-low values (≤10^{-4} Ω-cm) is long. Further, the boron doping process is diffusion-based and hence the achievable thickness of heavy boron doping on un-patterned silicon wafers is limited to ~10 µm.

In this work, we employ a new wafer-level aluminum thermomigration process that is much faster than the slow diffusion-based degenerative boron doping. Aluminum can be thermomigrated against a temperature gradient into few hundreds of microns thick silicon within few tens of minutes [8]. Aluminum, like boron, is a p-type dopant that has a smaller radius than silicon. By depositing a layer of aluminum and thermomigrating in silicon, a very high concentration of aluminum doping can be achieved. Thus, a faster and a larger reduction in TCF is possible at wafer-level.

This was investigated by evaporating 200 Å of aluminum onto the surface of SiBARs fabricated on ~ 10^{-2} Ω-cm silicon. The required temperature gradient is created in a furnace by turning off one of the many coil heaters (Figure 8). The wafer is positioned in the furnace at the boundary of the hot and cold regions, with the aluminum deposited side facing away from the heat. The temperature gradient across the thickness of the wafer drives the aluminum to thermomigrate into the resonating silicon bulk. Residual aluminum on the surface was removed using hydrofluoric acid after the thermomigration process. After one hour of

thermomigration in nitrogen ambient, the TCF of the SiBAR reduces by 24 ppm/°C from −27.8 ppm/°C to −3.8 ppm/°C (Figure 9).

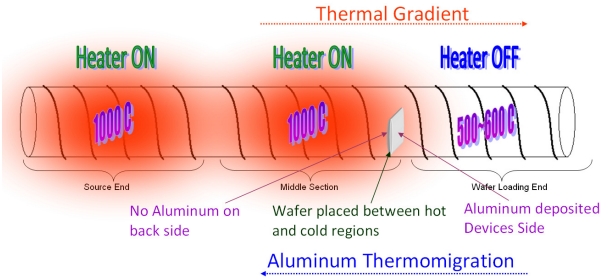

Fig 8: Wafer-level aluminum thermomigration process.

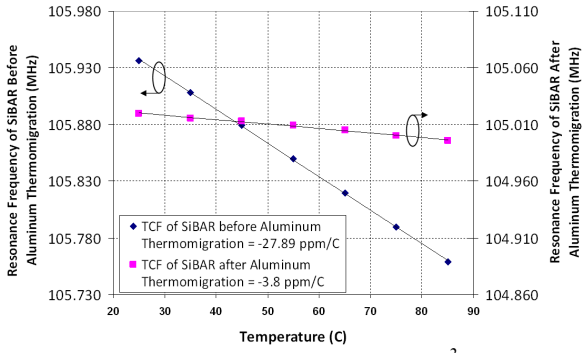

Fig. 9: Wafer-level TCF reduction in ~10^{-2} Ω-cm SiBAR after one hour of aluminum thermomigration.

The large thermal gradient across the thickness of the wafer induces stress which worsens with the rapid thermomigration of aluminum. As a result, some structural damage to the surface of the SiBAR was observed. However, CBARs withstand such induced stress (Figure 10) and continue to show a high Q. Thermomigration was also performed on CBARs reported in Figure 6 with a starting resistivity of ~10^{-3} Ω-cm. Upon thermomigration for 30 minutes, the TCF of the CBAR reduces from −6.31 ppm/°C to −3.63 ppm/°C (Figure 11) while retaining a Q of 40,000 in vacuum, which corresponds to an fQ of 4×10^{12} (Figure 12).

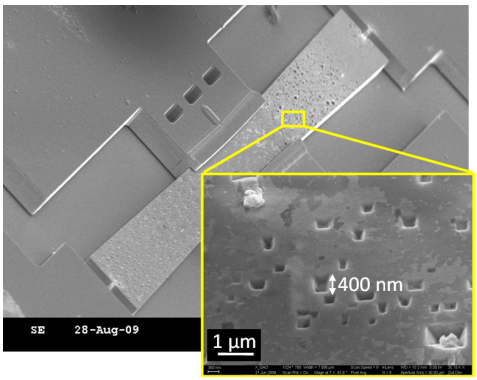

Fig. 10: Structural damage in a CBAR due to induced stress from 30 minutes of aluminum thermomigration.

CONCLUSION

Passive TCF compensation has been demonstrated in high quality factor silicon micromechanical resonators via engineering the geometry and material properties of the resonator. At a resistivity of ~10^{-3} Ω-cm, a SiBAR TCF of −21.46 ppm/°C reduces to −6.31 ppm/°C with a CBAR geometry, and is further reduced to −3.63 ppm/°C with 30 minutes of aluminum thermomigration.

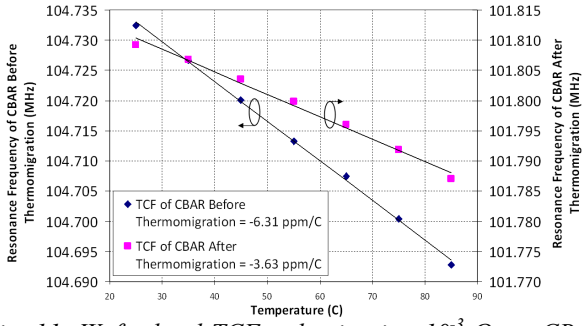

Fig. 11: Wafer-level TCF reduction in ~10^{-3} Ω-cm CBAR after 30 minutes of aluminum thermomigration.

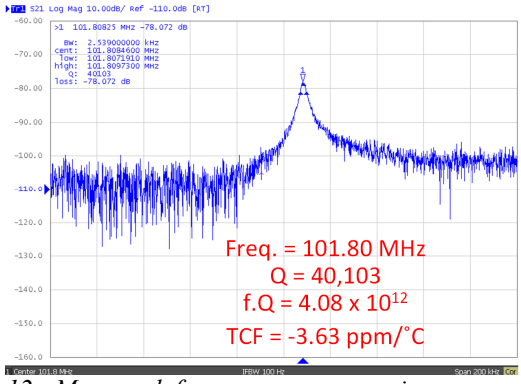

Fig. 12: Measured frequency response in vacuum of a ~10^{-3} Ω-cm CBAR after 30 minutes of aluminum thermomigration.

ACKNOWLEDGEMENTS

This work was supported by Integrated Device Technology (IDT), Incorporated.

REFERENCES

[1] S. Pourkamali, et al., "Low-Impedance VHF and UHF Capacitive Silicon Bulk Acoustic Wave Resonators—Part I: Concept and Fabrication," *IEEE Trans. Electron Devices,* vol. 54, no. 8, pp. 2017-2023, 2007.

[2] R. Abdolvand, et al., "Thin-film piezoelectric-on-silicon resonators for high-frequency reference oscillator applications," *IEEE Transactions on Ultrasonics, Ferroelectrics and Frequency Control*, vol. 55, no. 12, pp. 2596-2606, 2008.

[3] W.-T. Hsu, et al., "Stiffness-Compensated Temperature-Insensitive Micromech. Resonators," *IEEE MEMS*, Jan. 2002, pp. 731–734.

[4] J. S. Wang, et al., "Low-Temperature Coefficient Bulk Acoustic Wave Composite Resonators," *Appl. Phys. Lett.*, v. 40, no. 4, pp. 308– 310, 1982.

[5] R. Melamud, et al., "Temperature-Compensated High-Stability Silicon Resonators," *Appl. Phys. Lett.*, vol. 90, no. 24, pp. 1-3, 2007.

[6] A. K. Samarao, et al., "Temperature Compensation of Silicon Micromechanical Resonators via Degenerate Doping," *IEEE International Electron Devices Meeting*, Dec 2009.

[7] P. Csavinszky, et al., "Effect of Doping on Elastic Constants of Silicon," *Physical Review*, vol. 132, no. 6, pp 2434-2440, 1963.

[8] C. C. Chung, et al., "Thermomigration-based junction isolation of bulk silicon MEMS devices," *JMEMS,* vol. 15, no. 5, pp 1131-1138, 2006.